Vol. 58: 95–107, 2009
doi: 10.3354/ame01359

AQUATIC MICROBIAL ECOLOGY
Aquat Microb Ecol

Printed December 2009
Published online December 8, 2009

OPEN ACCESS

Temporal changes of major bacterial groups and bacterial heterotrophic activity during a *Phaeocystis globosa* bloom in the eastern English Channel

D. Lamy[1,4,5,*], I. Obernosterer[2,3], M. Laghdass[1,2,3], L. F. Artigas[1], E. Breton[1], J. D. Grattepanche[1], E. Lecuyer[1], N. Degros[1], P. Lebaron[2,3], U. Christaki[1]

[1]Univ Lille Nord de France, ULCO, LOG, 32. Av. Foch and CNRS, UMR 8187, 62930 Wimereux, France
[2]UPMC Univ Paris 06, UMR 7621, LOBB, Observatoire Océanologique, 66651 Banyuls-sur-Mer, France
[3]CNRS, UMR 7621, LOBB, Observatoire Océanologique, 66651, Banyuls-sur-Mer, France

[4]*Present address:* Department of Biological Oceanography, Royal Netherlands Institute for Sea Research, PO Box 59, 1790 AB, Den Burg, Texel, The Netherlands

[5]*Present address:* Department of Marine Biology, University of Vienna, Althanstrasse 14, 1090 Vienna, Austria

ABSTRACT: The temporal changes in major bacterial groups and bulk heterotrophic activity were determined during the growth, senescence and post-bloom phases of a *Phaeocystis globosa* bloom, at a coastal site in the eastern English Channel. Cell-specific exoenzymatic activities were highest during the growth period of *P. globosa*, while bacterial abundance and bacterial heterotrophic production peaked during the senescence of the *P. globosa* bloom. *Bacteroidetes* and *Gammaproteobacteria* were the most important bacterial groups during the growth period of *P. globosa*, contributing between 13 and 47% of bulk bacterial abundance and leucine incorporation. At the end of the phytoplankton growth period, *Gammaproteobacteria* were the most important contributors to bacterial heterotrophic production, accounting for 68% of bulk leucine incorporation. During the senescent phase, 36 and 29% of bulk leucine incorporation were attributable to *Bacteroidetes* and *Alphaproteobacteria*, respectively. Finally, after the disappearance of the bloom, *Gamma-* and *Alphaproteobacteria* dominated by the *Roseobacter* clade were responsible for 33 and 43% of bulk leucine incorporation, respectively. The relative abundance of the bacterial groups showed little variability between consecutive dates during most of the study period. The contributions of different bacterial groups to bulk abundance and leucine incorporation were correlated with exo-proteolytic and -glucosidic activities and with particulate organic carbon, suggesting at least some specificity of these bacterial groups with respect to their metabolic properties in the environment.

KEY WORDS: Bacterial succession · MICRO-FISH · Bacterial activity · *Phaeocystis globosa* · Eastern English Channel · SOMLIT

INTRODUCTION

Heterotrophic bacteria contribute significantly to the cycling of matter and energy in marine systems, as demonstrated by measurements of their bulk abundance, production and respiration, and, more specifically, of their enzymatic activities (Chrost 1991, Robinson 2008, Sherr & Sherr 2008). It is also well established that marine bacteria are phylogenetically and phenotypically diverse (Giovannoni & Rappé 2000, Fuhrman & Hagstrom 2008). How and why specific bacterial communities dominate in a given environment, how they contribute to the cycling of nutrients, and by what parameters they are controlled remain open and fundamental ecological questions. Temporal changes in the bacterial community composition occur on seasonal scales (Fuhrman et al. 2006, Alonso-Saez & Gasol 2007, Lami et al. 2009), but pronounced shifts in bacterial diversity can also occur on shorter time scales, for example, during phytoplankton blooms (Fandino et al. 2001, Pinhassi et al. 2004, Brussaard et al. 2005, Alderkamp et al. 2006). Several recent studies have examined the spatial and temporal variability of both the presence and the metabolic activity of differ-

*Email: lamyd2@univie.ac.at

ent bacterial groups (Cottrell & Kirchman 2003, Alonso-Saez & Gasol 2007, West et al. 2008). However, little attention has been paid to the changes in bacterial community composition in relation to specific processes such as exo-enzymatic activities (Kirchman et al. 2004, Langenheder et al. 2006). Thus, questions as to whether the observed shifts in bacterial community composition reflect changes in bacterial metabolic functions remain poorly understood.

Phytoplankton blooms dominated by *Phaeocystis globosa* (Prymnesiophyceae) are recurrent events in many marine environments, in particular in the North Sea (Cadee & Hegeman 2002). This micro-algae, which is known to occur in a colonial form, is of particular interest due to its production of dimethylsulfoniopropionate (DMSP) (Liss et al. 1994) and also its massive release of organic matter during the decline of the bloom (Van Boekel et al. 1992). This latter phenomenon often results in foam accumulation on the coast (Lancelot 1995, Hubas et al. 2007). In the eastern English Channel, the spring algal community is typically dominated by *P. globosa*, with biomasses as high as 500 µg C l^{-1} (Breton et al. 2000, 2006). A few studies have thus far investigated the bacterial community present and active during a *P. globosa* bloom in the coastal North Sea (Brussaard et al. 2005, Alderkamp et al. 2006, Alonso & Pernthaler 2006a,b). Alderkamp et al. (2006) revealed that *Bacteroidetes* were an abundant and active group over the course of the bloom. The *Roseobacter* clade, one of the major lineages of *Alphaproteobacteria*, was observed to dominate microbial uptake of glucose and leucine before and during the *P. globosa* bloom in coastal North Sea waters (Alonso & Pernthaler 2006a,b). The aim of our study was to follow shifts in bulk bacterial abundance, heterotrophic production and exo-enzymatic activities along with bacterial community composition in relation to a set of environmental parameters during 3 contrasting phases of the *P. globosa* bloom (growth, senescence and post-bloom phases). We presumed that the massive input of organic matter supplied by *P. globosa* at our coastal site would result in pronounced changes in the bacterial community composition. Our hypothesis was that shifts in bulk bacterial abundance, community composition and leucine incorporation would be relatable to the growth, senescent and post-bloom phases of the *P. globosa* spring bloom in a coastal area of the eastern English Channel.

MATERIALS AND METHODS

Sampling site. Water samples were collected at the coastal station (50° 40′ 75 N, 1° 31′ 17 E; <25 m water depth) of the SOMLIT network (Service d'Observation du Milieu Littoral) in the eastern English Channel. The eastern English Channel is characterized by its tidal range, between 3 and 9 m, and a residual circulation parallel to the coast, with nearshore coastal waters drifting from the English Channel into the North Sea. This coastal site is influenced by freshwater run-off from the Seine estuary. This so-called 'coastal flow' (Brylinski et al. 1991) is separated from offshore waters by a tidally maintained frontal area (Brylinski & Lagadeuc 1990). Sampling was always carried out at low tide. Sub-surface sampling (1 m water depth) was conducted once every 1 or 2 wk from February to mid-June 2007.

Physico-chemical parameters. Seawater temperature (T, °C) and salinity (S) were measured using a conductivity–temperature–depth profiling system (CTD Seabird SBE 25).

Nutrient concentrations were determined from 100 ml samples with an Alliance Integral Futura Autoanalyser II for nitrate (NO_3^-), nitrite (NO_2^-) and silicate [$(SiO_4)^{4-}$] (Mullin & Riley 1955a,b). Phosphate (PO_4^{3-}) concentration was determined manually according to Strickland & Parsons (1972) and Aminot & Kerouel (2004).

Particulate organic carbon (POC) was analysed by filtering (<150 mm Hg) duplicate 50 to 200 ml seawater samples through pre-combusted (4 to 5 h at 480°C) glass fibre filters (Whatman GF/F, 25 mm). Analysis was performed on a NA2100 Frisons CHN analyser after drying filters at 60°C for 24 h and exposure to HCl 1 N vapours for 5 h.

Samples for dissolved organic carbon (DOC) were filtered immediately after collection through pre-combusted GF/F filters and stored at –20°C in glass vials previously treated with HCl 10%, washed with MilliQ-water and pre-combusted at 480°C. Before analysis, filtrates were acidified to pH < 2 (HCl 6 N) and bubbled for 3 min with high-purity air (Suratman et al. 2009) to remove the dissolved inorganic carbon. Analyses employed a Shimadzu TOC Analyser 5000A using the high temperature catalytic oxidation (HTCO) method (Benner & Strom 1993, Cauwet 1994).

Phytoplankton parameters. Chlorophyll *a* (chl *a*) concentrations were estimated from 0.5 to 1 l water samples following Strickland & Parsons (1972). Samples were vacuum filtered on Whatman GF/F glass-fibre filters, which were immediately stored at –20°C in the dark until processing. Chlorophyll pigments from ground filters were extracted in 90% acetone overnight at 4°C. Chl *a* concentrations in the extracts were determined following Yentsch & Menzel (1963) using a 10-AU Turner Designs fluorometer.

Phytoplankton floristic analysis employed fixed samples (1% Lugol-glutaraldehyde solution in final concentration) examined using inverted microscopy

(Nikon TE2000-S) after sedimentation in 10 ml Hydrobios chambers. Diatom carbon biomass was calculated on the basis of cell concentration and specific biometry using the size-dependent relationship recommended by Menden-Deuer & Lessard (2000). Carbon biomass of the *Phaeocystis globosa* colony was calculated from biovolume measurements at ×100 or ×200 magnification, as previously described by Breton et al. (2006). Carbon biomass of *P. globosa* colonial and flagellate free-living cells were estimated by counts at ×400 magnification, and by applying carbon conversion factors of 14.2 and 8 pg C cell^{-1}, respectively (Schoemann et al. 2005).

Bacterioplankton abundance, production and exoenzymatic activities. Sub-samples for bacterial counts were immediately preserved in borate-buffered 0.2 µm pre-filtered formalin (3% final concentration) and stored at 4°C. Bacteria were enumerated by the epifluorescence direct counting method (Leica Leitz DMR; 365 nm) after DAPI staining (4 µg ml^{-1}, final concentration) following Porter & Feig (1980). A minimum of 500 cells filter^{-1} was counted in at least 10 randomly selected fields.

Total bacterial production was estimated from the rates of ^{3}H-leucine incorporation (Kirchman et al. 1985). Samples of 10 ml (3 replicates and 2 formalin-killed blanks) were incubated in the dark at *in situ* surface temperature for 1.5 h using 20 nM ^{3}H-leucine as a final saturation concentration. Kinetic experiments were previously run to (1) ensure that the concentration of added radiotracer was sufficient to prevent isotope dilution problems and (2) determine the incubation time for the *in situ* level of activity. After incubation, samples were extracted with ice-cold trichloroacetic acid (TCA; 5% final concentration) at 0°C for 20 min and filtered onto 0.2 µm polycarbonate filters (Millipore Nucleopore, 25 mm diameter). The radioactivity associated with the filters was measured with a liquid scintillation counter (Wallak 14, Perkin Elmer). Bacterial carbon production (BP; in g C l^{-1} h^{-1}) was calculated according to Kirchman et al. (1993).

The potential exoproteolytic and exoglucosidic activities (EPA and EGA, respectively) were assayed using fluorogenic substrate analogues (Hoppe 1993) derived from 7-amino-4-methyl-coumarin (AMC) and 4-methylumbelliferone (MUF), respectively. Exoproteolytic activity (EPA) was assayed as the hydrolysis rate of leucine-AMC (leu-AMC), whereas exoglucosidic activity (EGA) was assayed using MUF-β-D-glucopyranoside (MUF-G). After substrate addition (1000 µM leu-AMC and 1000 µM MUF-G) 4 ml triplicates were incubated at *in situ* temperature in the dark for 5 h for EPA and 8 h for EGA. Controls in duplicates were run adding 0.4 ml of stopper solutions (sodium dodecyl sulphate 10% and formaldehyde 37% for EPA and EGA, respectively) before substrate addition. Kinetic experiments were carried out to verify the linearity of the reaction during the incubation periods and to determine the saturating substrate concentrations during the sampling period. The EPA was determined as the rate of AMC, while the EGA was determined as the rate of MUF production. Fluorescence was measured using a Hitachi F2500 spectrofluorometer (excitation: emission of 380:440 nm for AMC and 364:460 nm for MUF) previously calibrated with standard solutions of AMC and MUF. Cell-specific exoproteolytic and exoglucosidic activities (EPAsp and EGAsp, respectively, in amol cell^{-1} h^{-1}) were calculated as ratios of exoenzymatic activities and total bacterial abundance.

Heterotrophic nanoflagellate abundance. To enumerate heterotrophic nanoflagellates (HNF), 5 ml samples were fixed with formaldehyde at a final concentration of 2%. Samples were filtered onto black Nuclepore filters (pore size: 0.8 µm) then stained with DAPI (Porter & Feig 1980) within 5 h of sampling and stored at –20°C until counting. Filters were mounted on slides, and HNF were enumerated using a LEITZ DMRB epifluorescence microscope at ×1000. Autotrophic and heterotrophic nanoflagellates were distinguished based on chlorophyll autofluorescence under blue light excitation.

FISH and MICRO-FISH experiments. Fluorescence *in situ* hybridisation (FISH) with rRNA-targeted oligonucleotide probes followed Glöckner et al. (1996), using Cy3-labeled probes. The probes employed were Eub338-I, -II and -III (target most *Bacteria*; Amann et al. 1990, Daims et al. 1999), Pla886 (targets most *Planctomycetales*; Neef et al. 1998), Arch915 (targets some *Archaea*; Stahl & Amann 1991), Alf968 (targets most *Alphaproteobacteria*; Amann et al. 1997), Bet42a and Gam42a (target most *Beta-* and *Gammaproteobacteria*, respectively; Manz et al. 1992), CF319a (targets many groups belonging to the *Bacteroidetes*; Manz et al. 1996), Ros537 (targets members of the *Roseobacter–Sulfitobacter–Silicibacter* group; Eilers et al. 2001) and SAR11-441R (targets the SAR11 cluster from *Alphaproteobacteria*; Morris et al. 2002). Unlabeled competitor probes were used for *Betaproteobacteria* and *Gammaproteobacteria* (Manz et al. 1992). A negative probe (the Eub antisense probe Non338) was used to determine non-specific binding (Glöckner et al. 1999) and never exceeded 5% of DAPI counts.

For microautoradiography FISH (MICRO-FISH) experiments, raw seawater samples (5 ml) were incubated with ^{3}H-leucine (20 nM final concentration, specific activity 170 Ci mmol^{-1}; Perkin Elmer) at *in situ* temperature in the dark for 1.5 h (Lee et al. 1999, Ouverney & Fuhrman 1999). Paraformaldehyde (PFA, 2% final concentration) was added to controls 15 min

prior to the addition of the radioactive compound. After incubation, samples were fixed with PFA (2% final conc.) and stored at 4°C overnight. Fixed samples were then filtered onto 0.2 µm pore-size polycarbonate filters, which were then kept at –20°C until FISH analysis (Glöckner et al. 1996). Following FISH of the bacterial cells, individual cell activity was determined by microautoradiography as described in Cottrell & Kirchman (2003). In a dark room, slides were dipped in a 43°C tempered photographic emulsion (KODAK NTB-2 diluted to half strength with 43°C pre-warmed deionised water). The filters were then placed on the slides, with the cells facing toward the emulsion. The slides were placed on an ice-cold bar for 15 min to solidify the emulsion before being transferred to black boxes at 4°C for 24 h until development. The optimal exposure time was determined by time series experiments for the dates when bacterial heterotrophic production showed the lowest and the highest values, respectively. Emulsion was developed in a 14°C tempered Dektol developer (Kodak D19) for 2 min, a 14°C deionised water stop bath for 10 s and a 14°C tempered fixer (Kodak T-Max) for 6 min. The slides were then rinsed in water for 6 min, dipped for 2 min in 1% glycerol and dried overnight in a vacuum desiccant chamber in the dark. Filters were peeled away from the emulsion, and the cells embedded onto the emulsion were stained with an antifading mounting medium (4:1 mixture of Citifluor and Vectashield) containing 0.5 ng μl^{-1} DAPI. Total number of cells (DAPI cells), cells affiliated with a specific bacterial group (Cy3 labeled) and cells that assimilated the radiolabeled compound (with silver grains) were counted using semi-automated microscopy (Olympus Provis AX70) and image analysis (ImagePro) as described by Cottrell & Kirchman (2003). Data were collected from 10 view fields with at least 500 cells $sample^{-1}$. The proportion of DAPI cells that are leucine active were determined as the fraction of total DAPI-stained cells with silver grains. The composition of the active community (percent of leucine-active cells) was determined as the fraction of cells with silver grains that are probe positive.

Statistical analyses. The relative abundance and activities of the major bacterial groups were compared: (1) within a date/among groups and (2) within a group/among dates, using an analysis of variance (ANOVA) test followed by the Newman-Keuls (SNK) *a posteriori* test on a log-normalized data set. The homogeneity of the variance was verified on a log-normalized data set (Bartlett test, $p < 0.05$). The comparison between the relative contribution of *Roseobacter* and SAR11 to bacterial abundance and activity was done using a unilateral Student's *t*-test on log-normalized data. A regression analysis was conducted of the relative contribution of a bacterial group to DAPI-stained cells and to leucine-active cells for each bacterial group. Only the significant regressions are shown. The slopes of the significant regressions were compared amongst themselves and with the slope 1:1 using a Student's *t*-test. Spearman correlations were performed to identify statistically significant relations between the targeted bacterial groups and biotic and abiotic parameters. A cluster analysis was applied to analyze the variability in the abundance and activity of major bacterial groups among samples (Bray-Curtis similarity measure and group average). The similarity among samples was calculated based on the relative abundance of each bacterial group and the relative contribution of each bacterial group to leucine incorporation. An analysis of similarities (ANOSIM) was conducted on the percent of DAPI cells and the percent of leucine-active cells of each targeted bacterial group. Samples were grouped according to the 3 periods of the *Phaeocystis globosa* bloom (growth, senescence and post-bloom). ANOSIM provides a way to test whether the differences observed among the bacterial between the 3 periods were significant. The data analyses were performed with XLSTAT Pro (Ver. 2006), SYSTAT 10 and PRIMER 6.

RESULTS

Physicochemical parameters

Surface water temperature gradually increased from 8.3°C on 19 February to 15.7°C on 14 June 2007 (Table 1). Surface water salinity averaged (±SD) 33.7 ± 0.4, and low values (<33.50) coincided with heavy rainfall (13 March, 11 April and 9 May; Table 1). Concentrations of inorganic nutrients were highest in March before the onset of the phytoplankton bloom [37.23 µM for $NO_3^- + NO_2^-$, 14.34 µM for $(SiO_4)^{4-}$, and 0.67 µM for PO_4^{3-}] and they dropped dramatically over the course of the study period (Table 1). DOC and POC concentrations increased from 176 to 444 µM, and from 15 to 140 µM, respectively, from mid-March to early May. Concentrations of DOC remained elevated until the end of May (319 µM), while the concentration of POC rapidly decreased and reached 23 µM by the end of May (Table 1).

Phytoplankton bloom succession

Diatoms and *Phaeocystis globosa* alternated in dominance, representing 4.2 to 99.1% and 0.0 to 99.7% of the phytoplankton biomass, respectively. They dominated the phytoplankton biomass by an average (±SD) of 94.3 ± 13.4% (n = 12, range: 54.5 to 99.9%). Other

Table 1. Temperature (Temp.), salinity (S), concentrations of inorganic nutrients [NO^{3-}, nitrates; NO^{2-}, nitrites; $(SiO_4)^{4-}$, silicate; PO_4^{3-}, phosphate], dissolved organic carbon (DOC) and particulate organic carbon (POC) during the study period in 2007

Sampling date	Temp. (°C)	S	$NO_3^- + NO_2^-$ (µM)	$(SiO_4)^{4-}$ (µM)	PO_4^{3-} (µM)	DOC (µM)	POC (µM)
19 Feb	8.3	34.1	23.07	11.57	0.77		26
13 Mar	9.5	32.7	37.23	14.34	0.67	178	15
27 Mar	8.8	33.4	18.30	3.21	0.21	194	26
2 Apr	9.3	33.7	11.36	2.84	0.09	176	37
11 Apr	10.0	33.4	4.08	1.37	0.14	254	53
17 Apr	10.6	33.9	4.68	2.19	0.06	237	71
2 May	12.6	33.9	5.30	0.84	0.07	243	140
9 May	13.1	33.3	2.84	2.69	0.46	444	103
15 May	13.3	34.0	0.11	1.27	0.06	316	38
24 May	14.0	34.1	0.28	1.42	0.05	400	58
31 May	14.6	34.1	0.51	1.60	0.05	319	23
14 Jun	15.7	34.3	0.51	2.54	0.03	256	29

phytoplankton groups present such as Cryptophyceae were a minor portion of the phytoplankton biomass, accounting for from 0.0 to 12.1% (mean ± SD: 1.8 ± 4.1%, n = 12). The phytoplankton bloom started by mid-March and was initially dominated by diatoms (biomass range: 22.7 to 264.5 µg C l^{-1}; Fig. 1a). *P. globosa* biomass (biomass range: 0.1 to 717.4 µg C l^{-1}) started to increase in early April (Fig. 1a) and dominated the bloom until the end of May. One exception was 9 May, when the *P. globosa* biomass equalled that of diatoms (221.1 µg C l^{-1}; Fig. 1a). This sudden decrease in *P. globosa* biomass coincided with a peak in ciliate biomass (105.2 µg C l^{-1}; J. D. Grattepanche unpubl. data). Concentrations of chl *a* steadily increased from mid-March (1.9 µg chl *a* l^{-1}) to the beginning of May (20.3 µg chl *a* l^{-1}) and rapidly decreased thereafter (Fig. 1a). The percentage of *P. globosa* cells considered colonial is indicative of the growth and senescent bloom phases (Rousseau et al. 2007). In the present study, the growth phase of the bloom lasted from mid-March to mid-April, and the duration of the senescent phase was from mid-April to the end of May (Fig. 1b).

Bacterial stocks and activity

Bacterial abundance increased progressively during the phytoplankton bloom from 0.5×10^6 cells ml^{-1} in February to 1.0×10^6 cells ml^{-1} in April (Fig. 2a). Bacterial heterotrophic production slightly increased from 8.1 ng C l^{-1} h^{-1} to values ranging between 26.2 and 62.1 ng C l^{-1} h^{-1} in April and early May. Both bacterial abundance and heterotrophic production were highest at the last sampling date (24 May) during the senescent phase (2.1×10^6 cells ml^{-1} and 179 ng C l^{-1} h^{-1}, respectively; Fig. 2a,b). At the end of May, both bacterial abundance and bacterial heterotrophic production rapidly declined to 0.8×10^6 cells ml^{-1} and 22.5 ng C l^{-1} h^{-1}, respectively, concurrent with the disappearance of *Phaeocystis globosa*. The abundance of HNFs increased with bacterial abundance during the growth phase of the bloom (from 1.9 to 13.9×10^3 cells ml^{-1}; Fig. 2a). At the end of the *P. globosa* bloom, the highest HNF abundance (15.5×10^3 cells ml^{-1}) coincided with low bacterial abundance and production (Fig. 2a). The percent of DAPI cells that were leucine active ranged between 15 and 35% and increased during the course of the bloom to a maximum value during the late stage of the senescence period of the *P. globosa* bloom (Fig. 2b); the temporal pattern closely followed that of bulk leucine incorporation (Fig. 2b), though the correlation was not significant (Spearman's r = 0.473, p = 0.142).

EPAsp and EGAsp increased markedly during the early stages of the phytoplankton bloom, reaching 239.1 and 37.3 amol $cell^{-1}$ h^{-1}, respectively (Fig. 2c). During the senescent phase, EPAsp was very variable and remained relatively high (>100 amol $cell^{-1}$ h^{-1}) while EGAsp decreased to values between 3.5 and 13.1 amol $cell^{-1}$ h^{-1}.

Relative abundance of major bacterial groups

Bacteria dominated the heterotrophic prokaryotic community during the whole study period, accounting for from 52 to 82% (n = 11) of the DAPI-stained cells and for from 61 to 96% (n = 10) of the leucine-active DAPI cells. The relative contribution of *Archaea* represented 7 ± 5% (n = 11) and 8 ± 9% (n = 10) of the DAPI-stained cells and the leucine-active DAPI cells, respectively (data not shown). The sum of the bacterial groups targeted in the present study (*Alpha-*, *Beta-*, *Gammaproteobacteria* and *Bacteroidetes*) represented 73 ± 13% (n = 11) and 89 ± 26% of the DAPI-stained cells and the leucine-active DAPI cells, respectively. Preliminary FISH analyses revealed that *Planctomycetales* accounted for <0.4% of the DAPI-stained cells at our coastal site in the eastern English Channel, and thus will not be further discussed in the present study.

Bacteroidetes dominated the bacterial community during the entire study period (32 ± 11% of the DAPI-stained cells, n = 11; Fig. 3a). During the senescent phase of the *Phaeocystis globosa* bloom, their relative contribution was significantly higher than that of the other bacterial groups (ANOVA test for each date of the senescent

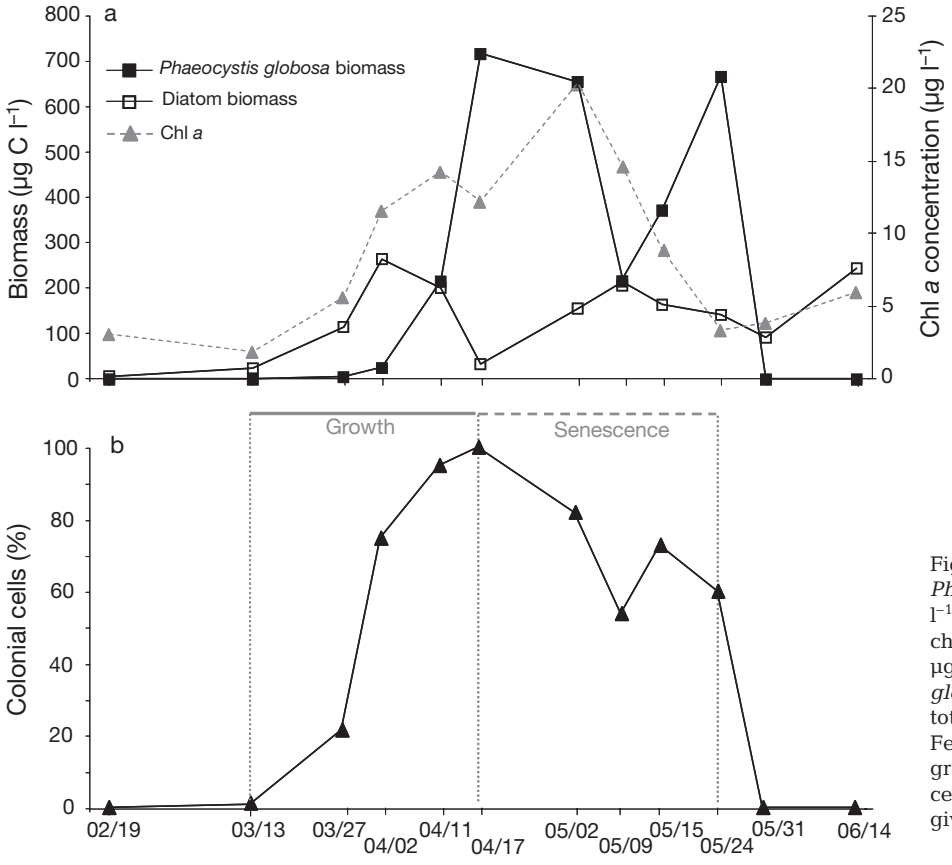

Fig. 1. Temporal changes in: (a) *Phaeocystis globosa* biomass (µg C l^{-1}), diatom biomass (µg C l^{-1}) and chlorophyll *a* concentration (chl *a*, µg l^{-1}) and (b) the percentage of *P. globosa* colonial cells among the total *P. globosa* cells (%) from 19 February to 14 June 2007. Periods of growth (continuous line) and senescence (dashed line) of *P. globosa* are given above the graph in (b). Dates are mm/dd

phase, except for 15 May, $p < 0.001$; SNK test, $p < 0.001$). The relative contribution of *Bacteroidetes* significantly declined after the senescent phase (ANOVA test, $p < 0.0001$; SNK test, $p < 0.001$) and contributed to about 20% of the DAPI-stained cells during the post-bloom phase (Fig. 3a). The relative contribution of *Alphaproteobacteria* did not change significantly during the study period (ANOVA test, $p = 0.607$) and accounted for 13 ± 4% ($n = 11$) of the DAPI-stained cells (Fig. 3a). Within the *Alphaproteobacteria*, *Roseobacter* dominated over SAR11 (Student's $t = 8.41$, $p < 0.0001$; Fig. 4a). *Roseobacter* comprised, on average, 12 ± 3% ($n = 9$) of the DAPI-stained cells during the course of the bloom, and represented up to 23% of the DAPI-stained cells following the senescent phase. The relative contribution of SAR11 varied between 0.1 and 8% of the DAPI-stained cells (3 ± 2%, $n = 11$; Fig. 4a). The ratio (*Roseobacter* + SAR11):*Alphaproteobacteria* in percent of DAPI cells ranged from 0.62 to 1.59 (1.18 ± 0.28). *Betaproteobacteria* had an overall contribution to the bacterial community similar to that of *Alphaproteobacteria* (12 ± 4%, $n = 10$; Fig. 3a), but the relative contribution of *Betaproteobacteria* increased significantly up to 30% during the post-bloom period (ANOVA test between growth, senescent and post-bloom phases, $p < 0.01$; SNK test, $p < 0.01$). The relative contribution of *Gammaproteobacteria* increased from 13% at the onset of the bloom to 30% during the peak of phytoplankton bloom. Their contribution was significantly higher during the growth phase than during the senescent and the post-bloom phases (ANOVA test, $p < 0.01$; SNK test, $p < 0.05$). During the latter 2 periods, *Gammaproteobacteria* accounted for from 5 to 16% of the DAPI-stained cells and their contribution did not change significantly over time (SNK test, $p = 0.72$).

Relative contribution of major bacterial groups to leucine incorporation

Bacteroidetes and *Gammaproteobacteria* dominated the active bacterial community during the growth period of *Phaeocystis globosa*, contributing to 33 ± 9% ($n = 4$) and 40 ± 18% ($n = 4$) of leucine-active cells, respectively (Fig. 3b). At the end of the *P. globosa* growth period, *Gammaproteobacteria* were the most important contributors to bacterial biomass production, accounting for 68% of the leucine-active cells (ANOVA test, $p < 0.01$; SNK test, $p < 0.01$). During the senescent phase, 36 ± 16% ($n = 4$) and 29 ± 9% ($n = 3$) of the leucine-active cells were *Bacteroidetes* and *Alphaproteobacteria*, respectively (Fig. 3b), dominating the active community (ANOVA test, $p < 0.01$; SNK

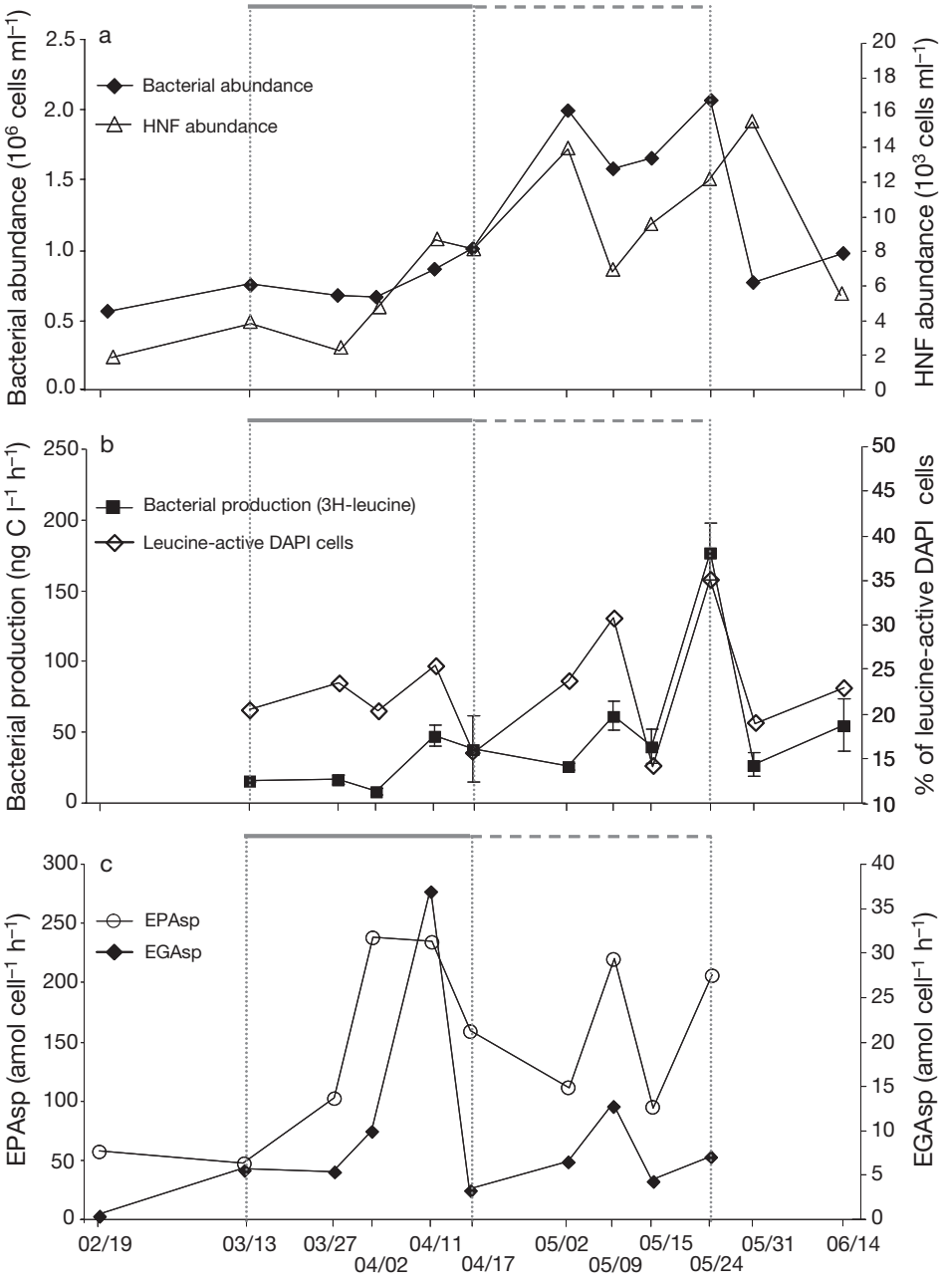

Fig. 2. Temporal changes in (a) bacterial abundance (10^6 cells ml^{-1}) and heterotrophic nanoflagellate abundance (HNF, 10^3 cells ml^{-1}), (b) bacterial heterotrophic production (ng C l^{-1} h^{-1}) and percent of DAPI cells that are leucine active (% of leucine-active DAPI cells) and (c) cell-specific exo-proteolytic activity (EPAsp, amol $cell^{-1}$ h^{-1}) and cell-specific exo-glucosidic activity (EGAsp, amol $cell^{-1}$ h^{-1}). Periods of growth (continuous line) and senescence (dashed line) of *Phaeocystis globosa* are given above each graph. Errors bars for bacterial production represent the standard deviation of triplicates. Dates are mm/dd

test, $p < 0.05$). One week after the disappearance of the bloom, *Gamma-* and *Alphaproteobacteria* were responsible for the bulk of leucine incorporation, accounting for 33 and 43% of the leucine-active cells, respectively (Fig. 3b). As for abundance, the relative contribution of *Roseobacter* to the active community (26 ± 9% of leucine-active cells, n = 9) was significantly higher than that of SAR11 (7 ± 7% of leucine-active cells, n = 9; Fig. 4b) during the study period (Student's $t = 6.64$, $p < 0.0001$). Following the senescent phase, *Roseobacter* made a larger contribution to bulk leucine incorporation (46% of leucine-active cells). The ratio (*Roseobacter* + SAR11):*Alphaproteobacteria* in percent of leucine-active cells ranged from 0.62 to 3.33 (1.48 ± 0.82).

Statistical relationships among groups

Regression analysis indicated that 48% of the variation in the contribution of bacterial groups to leucine incorporation was explained by the relative abun-

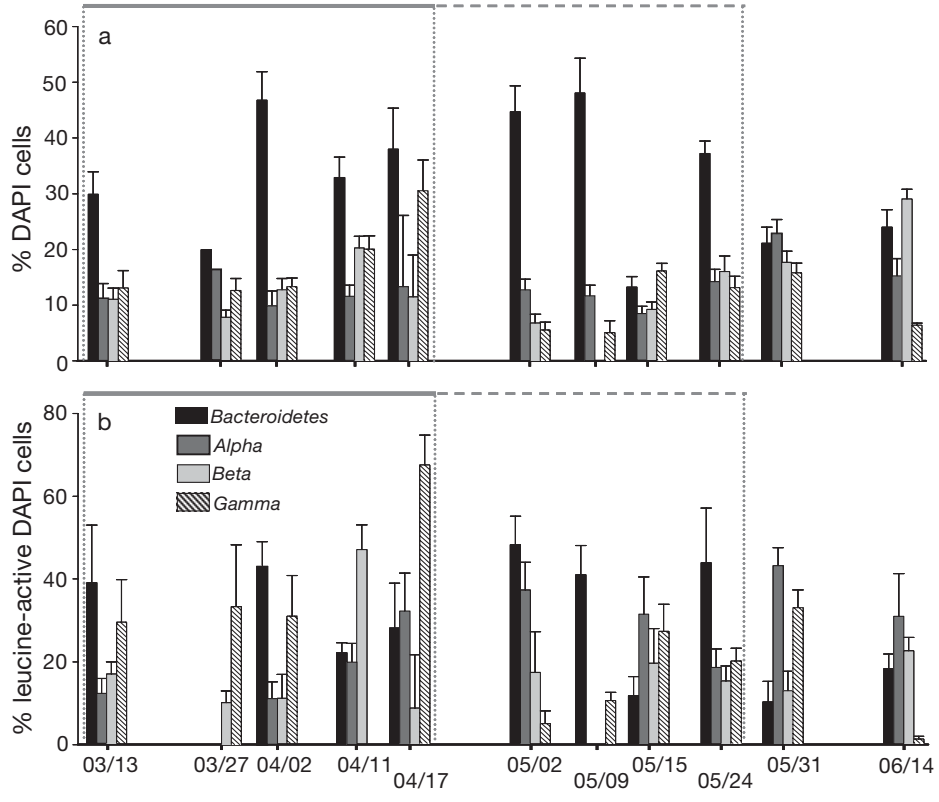

Fig. 3. Temporal changes in the relative contributions (in %) of *Bacteroidetes*, *Alpha-*, *Beta-* and *Gammaproteobacteria* to (a) the DAPI-stained cells and (b) the leucine-active DAPI cells. Periods of growth (continuous line) and senescence (dashed line) of *Phaeocystis globosa* are given above each graph. Errors bars represent standard deviation of 10 microscopic fields. Dates are mm/dd

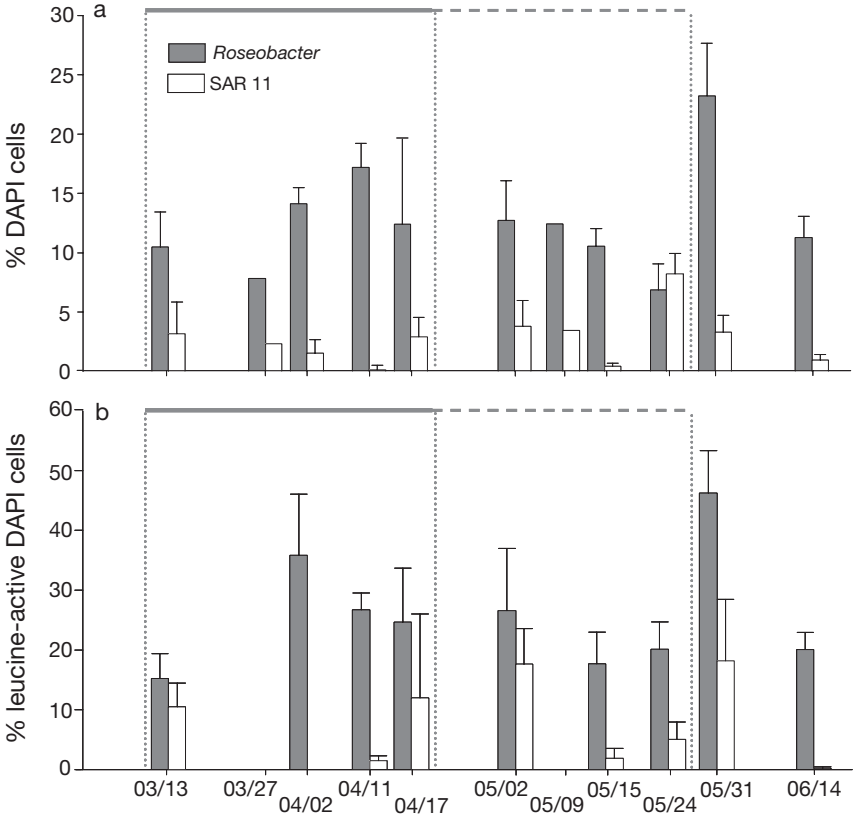

Fig. 4. Temporal changes in the relative contributions (in %) of *Roseobacter* and SAR11 to (a) the DAPI-stained cells and (b) the leucine-active DAPI cells. Periods of growth (continuous line) and senescence (dashed line) of *Phaeocystis globosa* are given above each graph. Errors bars represent standard deviation of 10 microscopic fields. Dates are mm/dd

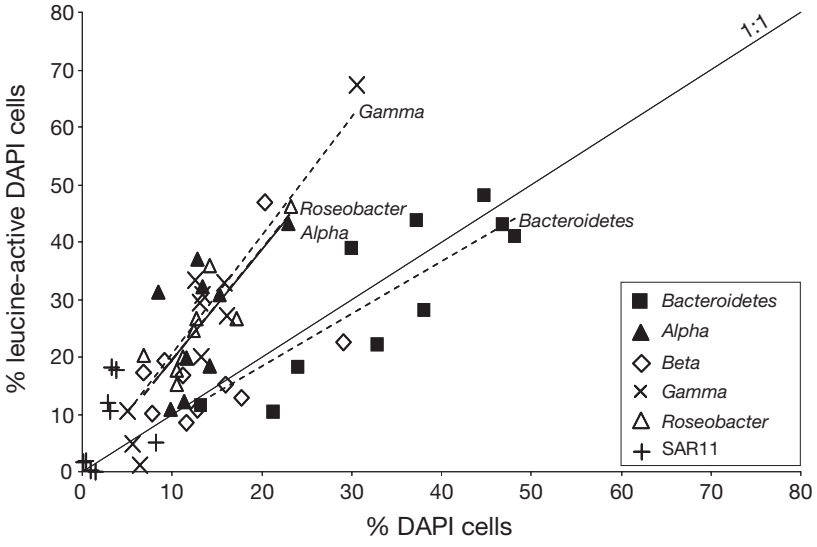

Fig. 5. Regression between the relative contribution of the targeted bacterial groups to the DAPI-stained cells and their relative contribution to the leucine-active DAPI cells. Lines are drawn for significant regressions

dance of the targeted bacterial groups (R^2 = 0.48; F = 51; p < 0.0001; Fig. 5). *Bacteroidetes* contributed to leucine incorporation in proportion to their relative contribution to abundance (slope comparison with slope 1:1, Student's t = 0.38, p < 0.001). In contrast, *Roseobacter* and *Gammaproteobacteria* made a higher contribution to bulk leucine incorporation than to bulk abundance (slope comparison with slope 1:1, Student's t = 2.52 and 3.41, respectively; p > 0.05; Fig. 5). The slopes of *Alphaproteobacteria* and *Roseobacter* were equal (slope comparison, Student's t = 0.01, p < 0.0001), indicating that the relative abundance and activity of *Roseobacter* paralleled the temporal pattern of *Alphaproteobacteria* (Fig. 5).

Links to environmental and bacterial parameters

The relative contribution of *Bacteroidetes* to bulk bacterial abundance was positively correlated with the EPAsp (Table 2; r = 0.68, p < 0.05) and with the concentration of POC (Table 2; r = 0.65, p < 0.05). In contrast, the relative contribution of *Bacteroidetes* to the active community did not correlate with any bacterial or environmental variable. The relative contribution of *Gammaproteobacteria* to the active community showed a strong negative relationship with the EGA (Table 2; r = –0.90, p < 0.01). The relative contribution of *Alphaproteobacteria* to the active community was positively linked to the abundance of HNFs (Table 2; r = 0.73, p < 0.05), and the relative contribution of *Roseobacter* to leucine incorporation showed a positive relationship with the EPAsp (Table 2; r = 0.86, p < 0.05).

To compare the bacterial communities in terms of the relative contribution to abundance and activity of the major bacterial groups, a cluster analysis with Bray-Curtis similarity was applied (Fig. 6). This analysis indicated that the samples from mid-March to early April (period of *Phaeocystis globosa* growth) and the sample from 24 May (period of *P. globosa* senescence) formed a cluster at 87% similarity (Fig. 6). *Bacteroidetes* were dominant at these dates (Fig. 3). Samples from the end of the growth period (11 and 17 April), when *Gammaproteobacteria* became more dominant in both abundance and activity, were grouped. Although less similar, the cluster grouping of samples from the senescent phase and the cluster grouping of post-bloom bacterial communities showed 76% similarity. Accordingly, the ANOSIM analysis showed that the differences between the periods tested (growth, senescence and post-bloom) were not higher than the differences within each period (R = 0.088, significance level of sample statistic = 35%). Thus, the periods did not drastically differ in terms of bacterial community composition or percent of leucine-active cells.

DISCUSSION

We observed changes in bulk bacterial parameters during a spring phytoplankton bloom dominated by *Phaeocystis globosa* in the eastern English Channel, accompanied by shifts in the abundance and the activ-

Table 2. Results of Spearman correlation analysis. Only significant correlations are shown. *Bacteroidetes* and *Alphaproteobacteria*: the relative contribution to the percent of DAPI cells of *Bacteroidetes* and *Alphaproteobacteria*, respectively; *leu-Gammaproteobacteria* and *leu-Roseobacter*: the relative contribution to the percent of leucine-active cells of *Gammaproteobacteria* and *Roseobacter*, respectively; POC: particulate organic carbon: EPAsp: cell-specific exoproteolytic activity; HNF: heterotrophic nanoflagellates; EGA: exoglucosidic activity

Variable 1	Variable 2	n	r	p
Bacteroidetes	POC	11	0.65	0.02
Bacteroidetes	EPAsp	9	0.68	0.04
Alphaproteobacteria	HNF	9	0.73	0.02
leu-Gammaproteobacteria	EGA	8	–0.90	0.002
leu-Roseobacter	EPAsp	7	0.86	0.014

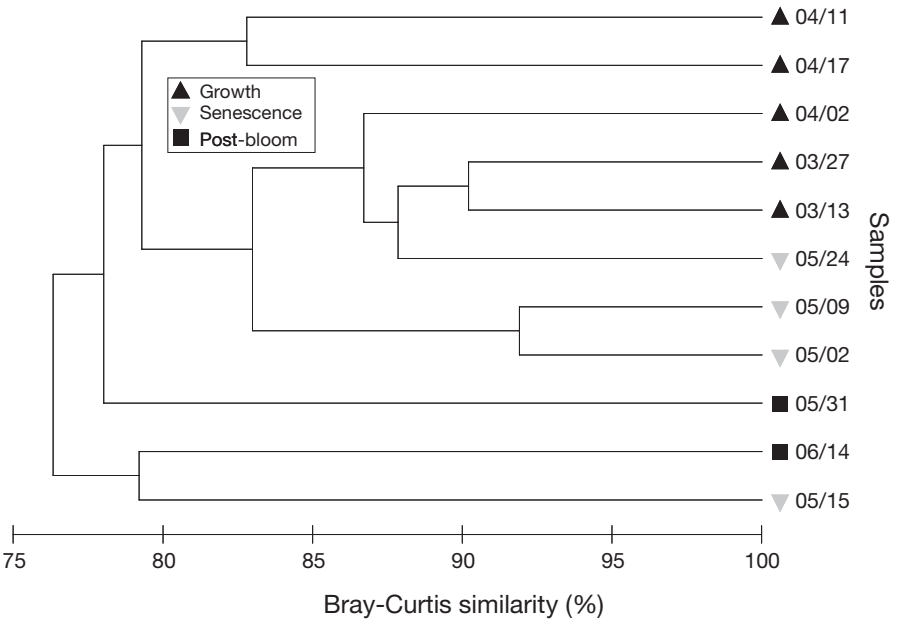

Fig. 6. Cluster analysis (Bray-Curtis similarity measure and group average) based on the relative abundance of each probe–stain contribution of the bacterial groups to DAPI-stained cells and to leucine-active cells. Dates are mm/dd. Samples are grouped by growth (black triangles), senescence (inverted grey trianlges) and post-bloom (black squares) periods of the *Phaeocystis globosa* bloom

ity of major bacterial groups. The different bacterial groups examined revealed contrasting temporal patterns (Figs. 3 & 4), linked to distinct bacterial and environmental parameters. Noteworthy was the finding that the contribution of the different bacterial groups to leucine incorporation was not always proportional to their contribution to abundance (Fig. 5). Results of the ANOSIM analysis indicted that the relative abundance and leucine incorporation of the bacterial groups did not change dramatically between consecutive dates. The senescent phase appeared to be the most variable one, but the similarity index remained high (up to 76%).

Bacteria belonging to the *Bacteroidetes* group dominated bacterial abundances and activities during the growth and senescent phases of the *Phaeocystis globosa* bloom (Fig. 3). The relative contribution of *Bacteroidetes* to bulk bacterial abundance was positively correlated to the EGA and to POC. This suggests that *Bacteroidetes* played a significant role in degradation of complex proteinaceous dissolved and particulate material. A similar conclusion was drawn in previous studies (Cottrell & Kirchman 2003, Bauer et al. 2006). Our results confirm those obtained during a 1 yr study in the coastal North Sea characterised by a *P. globosa* spring bloom (Alderkamp et al. 2006). These authors observed that *Bacteroidetes* comprised the most important fraction of the total prokaryotic community and showed the strongest increase in activity during the senescent stage of the bloom. *Bacteroidetes* were also important members in microbial enrichments degrading *Phaeocystis* sp. mucopolysaccharides (Janse et al. 2000, Brussaard et al. 2005). These observations suggest that *Bacteroidetes* likely play a major role in the degradation of organic matter produced in the *P. globosa* spring bloom. The *Flavobacteria*, which comprise the most abundant class of planktonic marine *Bacteroidetes* (Kirchman 2002), are reported to be colonisers of aggregates (Simon et al. 2002, Abell & Bowman 2005) and may occupy principally a 'particle-specialist' niche (Fandino et al. 2001). The strong positive correlation between *Bacteroidetes* and POC determined here suggests that particle-attached *Bacteroidetes* were most likely important in the dynamics of the prokaryotic community during the *P. globosa* bloom in the eastern English Channel. *Bacteroidetes* participated in leucine incorporation in proportion to their contribution to bulk abundance (Fig. 5). However, the lack of correlation between the relative contribution of *Bacteroidetes* to the active community and any of the variables measured in our study suggests complex interactions, possibly at a higher phylogenetic resolution than that considered here.

Gammaproteobacteria represented a lower proportion of the bacterial abundance than *Bacteroidetes* throughout the study period (<30%; Fig. 3a), but they significantly contributed to the leucine incorporation during 2 key periods of the *Phaeocystis globosa* bloom. *Gammaproteobacteria* contributed to 67 and 33% of the leucine-active cells at the end of the growth period (mid-April) and after the disappearance of the *P. globosa* bloom (end of May), respectively (Fig. 3b). In contrast to *Bacteroidetes*, the relative contribution of *Gammaproteobacteria* to the active community was

negatively correlated to the EGA. The high contribution of *Gammaproteobacteria* to bulk abundance and activity at the end of the *P. globosa* growth phase, when exoenzymatic activities were low, leads us to hypothesize that this group could efficiently metabolize readily available organic matter, either released from growing phytoplankton cells (Giovannoni & Rappé 2000) or supplied by another bacterial group through enzymatic activities. Members of the SAR86 cluster are cosmopolitan members of the *Gammaproteobacteria*, and they are abundant in the free-living communities of marine bacterioplankton (Acinas et al. 1999). In the coastal North Sea subject to *P. globosa* spring blooms, Alderkamp et al. (2006) observed a low but persistent fraction of SAR86 (range: 0 to 13%) throughout the season. Despite their low abundance, SAR86 contributed up to 60% of the bacterial biomass production during the *P. globosa* bloom (Alderkamp et al. 2006), similar to the results obtained in the present study for *Gammaproteobacteria*.

Bacteria belonging to the *Alphaproteobacteria* represented a small fraction of the bacterial assemblage over the study period (Fig. 3a), but contributed to 63% of the active cells after the senescent phase of the bloom (Fig. 3b). The low contribution of *Alphaproteobacteria* to bulk bacterial abundance despite their high activity (Fig. 5) suggests that top-down control, such as grazing, could be important in controlling the dynamics of this group through the preferential consumption of active cells (Jürgens et al. 1999, Sherr et al. 2002). The significant positive correlation between the relative contribution of *Alphaproteobacteria* to the active community and the abundance of HNFs supports this idea. Within the *Alphaproteobacteria*, *Roseobacter* clearly dominated over SAR11 throughout the study period in terms of both abundance and activity (Fig. 4). Moreover, the temporal evolution of *Roseobacter* in terms of abundance and activity followed that of *Alphaproteobacteria* (Fig. 5). The ratio (*Roseobacter* + SAR11):*Alphaproteobacteria* comprised from 0.62 to 1.59 (1.18 ± 0.28) and 0.62 to 3.33 (1.48 ± 0.82) when calculated with the percentage of DAPI cells and leucine-active cells, respectively. Ratios of >1 are not surprising, since the alphaproteobacterial probe is less specific than the *Roseobacter* and SAR11 probes and does not include all the alphaproteobacterial lineages (Amann & Fuchs 2008). Previous studies report contrasting seasonal patterns for *Roseobacter* and SAR11 (Alonso-Saez & Gasol 2007, Teira et al. 2008). *Roseobacter*-like bacteria were previously associated with high primary production and algal blooms (Zubkov et al. 2001). The significant correlation we observed between the relative contribution of *Roseobacter* to the active community and the EPAsp suggests that they are important for protein degradation. This is in line with previous observations that *Roseobacter* are important consumers of amino acids freshly released from exoproteolytic activities, in particular during phytoplankton blooms (Alonso-Saez & Gasol 2007). In addition, *Roseobacter* members are key participants in the assimilation of DMSP (Zubkov et al. 2001) produced during *Phaeocystis globosa* blooms (Liss et al. 1994). The importance of *Roseobacter* in the present study is in accordance with the observations of Alderkamp et al. (2006); although not abundant, the *Roseobacter* clade was the most active group within the *Alphaproteobacteria* throughout the spring and summer seasons.

Betaproteobacteria represented a minor part of the bacterial community (a mean of 12% during the *Phaeocystis globosa* growth phase), except after the senescent period when the percent of *Betaproteobacteria* increase to 20 and 29% of the DAPI-stained cells (Fig. 3a). *Betaproteobacteria* also contributed to a small portion of the active cells (≤20%), except for one peak at the end of the *P. globosa* growth period (Fig. 3b). *Betaproteobacteria* are generally abundant in rivers and freshwater environments (Kirchman et al. 2005), but are also abundant in coastal waters. For example, Longnecker et al. (2006) reported that a relative contribution of *Betaproteobacteria* comprised between 0 and 20% of the DAPI and leucine-active cells at the basin station off the coast of Oregon, with a punctual burst of 40% of leucine-active cells. In the same study area, members of the OM43 clade of *Betaproteobacteria* were found to be among the dominant lineages during a diatom bloom (Morris et al. 2006).

Our results show important temporal changes of major bacterial groups in the course of a spring phytoplankton bloom dominated by *Phaeocystis globosa.* The relative contribution of the bacterial groups to bulk abundance and leucine incorporation did not reveal any drastic changes between consecutive dates, but differed with the distinct phases of the phytoplankton bloom. We observed that the relative contributions of different bacterial groups to bulk abundance and leucine incorporation were, in part, related to bulk proteolytic and glucosidic activities. This suggests some specificity of these bacterial groups with respect to their ecological roles in the environment.

Acknowledgements. We thank P. Catala and A. C. Marc for their assistance with laboratory analyses, and the captain and the crew of the RV 'Sepia II' and 'Côtes de la Manche'. The authors also thank the French monitoring network SOMLIT for oceanographic coastal data. This work was supported by the French national network SOMLIT and the regional CPER project. We also thank J. Dolan for critical reading of the manuscript and English corrections.

LITERATURE CITED

Abell GCJ, Bowman JP (2005) Colonization and community dynamics of class *Flavobacteria* on diatom detritus in experimental mesocosms based on Southern Ocean seawater. FEMS Microbiol Ecol 53:379–391

Acinas SG, Anton J, Rodriguez-Valera F (1999) Diversity of free-living and attached bacteria in offshore western Mediterranean waters as depicted by analysis of genes encoding 16S rRNA. Appl Environ Microbiol 65:514–522

Alderkamp AC, Sintes E, Herndl GJ (2006) Abundance and activity of major groups of prokaryotic plankton in the coastal North Sea during spring and summer. Aquat Microb Ecol 45:237–246

Alonso C, Pernthaler J (2006a) Concentration-dependent patterns of leucine incorporation by coastal picoplankton. Appl Environ Microbiol 72:2141–2147

Alonso C, Pernthaler J (2006b) *Roseobacter* and SAR11 dominate microbial glucose uptake in coastal North Sea waters. Environ Microbiol 8:2022–2030

Alonso-Saez L, Gasol JM (2007) Seasonal variations in the contributions of different bacterial groups to the uptake of low-molecular-weight compounds in northwestern Mediterranean coastal waters. Appl Environ Microbiol 73:3528–3535

Amann R, Fuchs BM (2008) Single-cell identification in microbial communities by improved fluorescence *in situ* hybridization techniques. Natl Rev 6:339–348

Amann RI, Krumholz L, Stahl DA (1990) Fluorescent-oligonucleotide probing of whole cells for determinative, phylogenetic, and environmental studies in microbiology. J Bacteriol 172:762–770

Amann R, Glockner FO, Neef A (1997) Modern methods in subsurface microbiology: *in situ* identification of microorganisms with nucleic acid probes. FEMS Microbiol Rev 20:191–200

Aminot A, Kerouel R (2004) Dissolved organic carbon, nitrogen, and phosphorus in the N–E Atlantic and the N–W Mediterranean with particular reference to non-refractory fractions and degradation. Deep-Sea Res I 51:1975–1999

Bauer M, Kube M, Teeling H, Richter M and others (2006) Whole genome analysis of the marine *Bacteroidetes* '*Gramella forsetii*' reveals adaptations to degradation of polymeric organic matter. Environ Microbiol 8:2201–2213

Benner R, Strom M (1993) A critical evaluation of the analytical blank associated with DOC measurements by high-temperature catalytic oxidation. Mar Chem 41:153–160

Breton E, Brunet C, Sautour B, Brylinski JM (2000) Annual variations of phytoplankton biomass in the eastern English Channel: comparison by pigment signatures and microscopic counts. J Plankton Res 22:1423–1440

Breton E, Rousseau V, Parent JY, Ozer J, Lancelot C (2006) Hydroclimatic modulation of diatom/*Phaeocystis* blooms in nutrient-enriched Belgian coastal waters (North Sea). Limnol Oceanogr 51:1401–1409

Brussaard CPD, Mari X, Van Bleijswijk JDL, Veldhuis MJW (2005) A mesocosm study of *Phaeocystis globosa* (Prymnesiophyceae) population dynamics. II. Significance for the microbial community. Harmful Algae 4:875–893

Brylinski JM, Lagadeuc Y (1990) L'interface eau côtière/eau du large dans le Pas-de-Calais (côte française): zone frontale. CR Acad Sci Paris 311:535–540

Brylinski JM, Lagadeuc Y, Gentilhomme V, Dupont JP and others (1991) Le 'fleuve côtier': un phénomène hydrologique important en Manche orientale (exemple du Pas de Calais). Oceanol Acta 11:197–203

Cadee GC, Hegeman J (2002) Phytoplankton in the Marsdiep at the end of the 20th century; 30 years monitoring biomass, primary production, and *Phaeocystis* blooms. J Sea Res 48:97–110

Cauwet G (1994) HTCO method for dissolved organic-carbon analysis in seawater—influence of catalyst on blank estimation. Mar Chem 47:55–64

Chrost R (1991) Environmental control of the synthesis and activity of aquatic microbial ectoenzymes. In: Chrost R (ed) Microbial enzymes in aquatic environments. Springer-Verlag, New York, p 29–59

Cottrell MT, Kirchman DL (2003) Contribution of major bacterial groups to bacterial biomass production (thymidine and leucine incorporation) in the Delaware estuary. Limnol Oceanogr 48:168–178

Daims H, Bruhl A, Amann R, Schleifer KH, Wagner M (1999) The domain-specific probe EUB338 is insufficient for the detection of all bacteria: development and evaluation of a more comprehensive probe set. Syst Appl Microbiol 22: 434–444

Eilers H, Pernthaler J, Peplies J, Glockner FO, Gerdts G, Amann R (2001) Isolation of novel pelagic bacteria from the German Bight and their seasonal contributions to surface picoplankton. Appl Environ Microbiol 67:5134–5142

Fandino L, Riemann L, Steward G, Long A, Azam F (2001) Variations in bacterial community structure during a dinoflagellate bloom analysed by DGGE and 16S rDNA sequencing. Aquat Microb Ecol 23:119–130

Fuhrman J, Hagstrom A (2008) Bacterial and archaeal community structure and its patterns. In: Kirchman DL (ed) Microbioal ecology of the oceans. Wiley-Liss, New York, p 45–90

Fuhrman JA, Hewson I, Schwalbach M, Steele J, Brown M, Naeem S (2006) Annually reoccurring bacterial communities are predictable from ocean conditions. Proc Natl Acad Sci USA 103:13104–13109

Giovannoni S, Rappé M (2000) Evolution, diversity and molecular ecology of marine prokaryotes. In: Kirchman DL (ed) Microbial ecology of the oceans. Wiley-Liss, New York, p 47–84

Glöckner FO, Amann R, Alfreider A, Pernthaler J, Psenner R, Trebesius K, Schleifer KH (1996) An *in situ* hybridization protocol for detection and identification of planktonic bacteria. Syst Appl Microbiol 19:403–406

Glöckner FO, Fuchs BM, Amann R (1999) Bacterioplankton compositions of lakes and oceans: a first comparison based on fluorescence *in situ* hybridization. Appl Environ Microbiol 65:3721–3726

Hoppe H (1993) Use of fluorogenic model substrates for extracellular enzyme activity measurement of bacteria. In: Kemp P, Sherr B, Sherr E, Cole J (eds) Handbook of methods in aquatic microbial ecology. Lewis Publishers, London, p 423–431

Hubas C, Lamy D, Artigas LF, Davoult D (2007) Seasonal variability of intertidal bacterial metabolism and growth efficiency in an exposed sandy beach during low tide. Mar Biol 151:41–52

Janse I, Zwart G, van der Maarel M, Gottschal JC (2000) Composition of the bacterial community degrading *Phaeocystis* mucopolysaccharides in enrichment cultures. Aquat Microb Ecol 22:119–133

Jürgens K, Pernthaler J, Schalla S, Amann R (1999) Morphological and compositional changes in a planktonic bacterial community in response to enhance protozoan grazing. Appl Environ Microbiol 65:1241–1250

Kirchman D, K'Nees E, Hodson R (1985) Leucine incorporation and its potential as a measure of protein synthesis and biomass by bacteria in natural aquatic systems. Appl Env

Microbiol 49:599–607
Kirchman DL (2002) The ecology of Cytophaga–Flavobacteria in aquatic environments. FEMS Microbiol Ecol 39: 91–100
Kirchman D, Keil R, Simon M, Welschmeyers N (1993) Biomass and production of heterotrophic bacterioplankton in the oceanic subarctic Pacific. Deep-Sea Res 40:967–988
Kirchman DL, Dittel AI, Findlay SEG, Fischer D (2004) Changes in bacterial activity and community structure in response to dissolved organic matter in the Hudson River, New York. Aquat Microb Ecol 35:243–257
Kirchman DL, Dittel AI, Malmstrom RR, Cottrell MT (2005) Biogeography of major bacterial groups in the Delaware Estuary. Limnol Oceanogr 50:1697–1706
Lami R, Ghiglione JF, Desdevises Y, West NJ, Lebaron P (2009) Annual patterns of presence and activity of marine bacteria monitored by 16S rDNA–16S rRNA fingerprints in the coastal NW Mediterranean Sea. Aquat Microb Ecol 54:199–210
Lancelot C (1995) The mucilage phenomenon in the continental coastal waters of the North Sea. Sci Total Environ 165:83–102
Langenheder S, Lindstrom ES, Tranvik LJ (2006) Structure and function of bacterial communities emerging from different sources under identical conditions. Appl Environ Microbiol 72:212–220
Lee N, Nielsen PH, Andreasen KH, Juretschko S, Nielsen JL, Schleifer KH, Wagner M (1999) Combination of fluorescent *in situ* hybridization and microautoradiography—a new tool for structure–function analyses in microbial ecology. Appl Environ Microbiol 65:1289–1297
Liss PS, Malin G, Turner SM, Holligan PM (1994) Dimethyl sulfide and *Phaeocystis*—a review. J Mar Syst 5:41–53
Longnecker K, Homen DS, Sherr EB, Sherr BF (2006) Similar community structure of biosynthetically active prokaryotes across a range of ecosystem trophic states. Aquat Microb Ecol 42:265–276
Manz W, Amann R, Ludwig W, Wagner M, Schleifer KH (1992) Phylogenetic oligodeoxynucleotide probes for the major subclasses of Proteobacteria—problems and solutions. Syst Appl Microbiol 15:593–600
Manz W, Amann R, Ludwig W, Vancanneyt M, Schleifer KH (1996) Application of a suite of 16S rRNA–specific oligonucleotide probes designed to investigate bacteria of the phylum cytophaga–flavobacter–bacteroides in the natural environment. Microbiology 142:1097–1106
Menden-Deuer S, Lessard EJ (2000) Carbon to volume relationships for dinoflagellates, diatoms, and other protist plankton. Limnol Oceanogr 45:569–579
Morris RM, Rappe MS, Connon SA, Vergin KL, Siebold WA, Carlson CA, Giovannoni SJ (2002) SAR11 clade dominates ocean surface bacterioplankton communities. Nature 420:806–810
Morris RM, Longnecker K, Giovannoni SJ (2006) Pirellula and OM43 are among the dominant lineages identified in an Oregon coast diatom bloom. Environ Ecol 8:1361–1370
Mullin JB, Riley JP (1955a) The colorimetric determination of silicate with special reference to sea and natural waters. Anal Chim Acta 12:162–176
Mullin JB, Riley JP (1955b) The spectrophotometric determination of nitrate in natural waters, with particular reference to seawater. Anal Chim Acta 12:464–480
Neef A, Amann R, Schlesner H, Schleifer KH (1998) Monitoring a widespread bacterial group: *in situ* detection of *Planctomycetes* with 16S rRNA–targeted probes. Microbiology 144:3257–3266
Ouverney CC, Fuhrman JA (1999) Combined microautoradiography—16S rRNA probe technique for determination of radioisotope uptake by specific microbial cell types *in situ*. Appl Environ Microbiol 65:1746–1752
Pinhassi J, Sala MM, Havskum H, Peters F, Guadayol O, Malits A, Marrase CL (2004) Changes in bacterioplankton composition under different phytoplankton regimens. Appl Environ Microbiol 70:6753–6766
Porter KG, Feig YS (1980) The use of DAPI for identifying and counting aquatic microflora. Limnol Oceanogr 25:943–948
Robinson C (2008) Heterotrophic bacterial respiration. In: Kirchman DL (ed) Microbial ecology of the oceans. Wiley-Liss, New York, p 299–334
Rousseau V, Chretiennot-Dinet MJ, Jacobsen A, Verity P, Whipple S (2007) The life cycle of *Phaeocystis*: state of knowledge and presumptive role in ecology. Biogeochemistry 83:29–47
Schoemann V, Becquevort S, Stefels J, Rousseau W, Lancelot C (2005) *Phaeocystis* blooms in the global ocean and their controlling mechanisms: a review. J Sea Res 53:43–66
Sherr E, Sherr B (2008) Understanding roles of microbes in marine pelagic food webs: a brief history. In: Kirchman DL (ed) Microbial ecology of the oceans. Wiley-Liss, New York, p 27–44
Sherr EB, Sherr BF, Verity PG (2002) Distribution and relation of total bacteria, active bacteria, bacterivory, and volume of organic detritus in Atlantic continental shelf waters off Cape Hatteras, NC, USA. Deep-Sea Res 49:4571–4585
Simon M, Grossart HP, Schweitzer B, Ploug H (2002) Microbial ecology of organic aggregates in aquatic ecosystems. Aquat Microb Ecol 28:175–211
Stahl D, Amann R (1991) Development and application of nucleic acid probes. In: Stackebrandt E, Goodfellow M (eds) Nucleic acid techniques in bacterial systematics. John Wiley & Sons, Chichester, p 205–248
Strickland J, Parsons T (1972) A practical handbook of seawater analysis. Bull Fish Res Board Can 167:1–310
Suratman S, Weston K, Jickells T, Fernand L (2009) Spatial and seasonal changes of dissolved and particulate organic C in the North Sea. Hydrobiologia 628:13–25
Teira E, Gasol JM, Aranguren-Gassis M, Fernandez A, Gonzalez J, Lekunberri I, Alvarez-Salgado XA (2008) Linkages between bacterioplankton community composition, heterotrophic carbon cycling and environmental conditions in a highly dynamic coastal ecosystem. Environ Microbiol 10:906–917
Van Boekel WHM, Hansen FC, Riegman R, Bak RPM (1992) Lysis-induced decline of a *Phaeocystis* spring bloom and coupling with the microbial foodweb. Mar Ecol Prog Ser 81:269–276
West NJ, Obernosterer I, Zemb O, Lebaron P (2008) Major differences of bacterial diversity and activity inside and outside of a natural iron-fertilized phytoplankton bloom in the Southern Ocean. Environ Microbiol 10:738–756
Yentsch CS, Menzel DW (1963) A method for the determination of phytoplankton chlorophyll and phaeophytin by fluorescence. Deep-Sea Res 10:221–231
Zubkov MV, Fuchs BM, Archer SD, Kiene RP, Amann R, Burkill PH (2001) Linking the composition of bacterioplankton to rapid turnover of dissolved dimethylsulphoniopropionate in an algal bloom in the North Sea. Environ Microbiol 3:304–311

Editorial responsibility: Karel Simek, Ceske Budejovice, Czech Republic

Submitted: April 28, 2009; Accepted: July 30, 2009
Proofs received from author(s): November 13, 2009